ACS Catalysis

RESEARCH ARTICLE

pubs.acs.org/acscatalysis

Influence of Fluoride Anions on the Acid−Base Properties of Mg/Al Mixed Oxides

Manuela C. I. Bezen, Cornelia Breitkopf, and Johannes A. Lercher*

Department of Chemistry and Catalysis Research Center, Technische Universität München, Lichtenbergstrasse 4, Garching 85748, Germany

Supporting Information

ABSTRACT: Mg/Al mixed oxides derived from layered double hydroxide precursors were modified with fluoride anions to probe their influence on acid−base and catalytic properties. Fluoride anions were incorporated by treatment with aqueous NH_4F. The structure of the precursors and the modified materials were analyzed by XRD, ^{27}Al NMR, and ^{19}F MAS NMR. The modification of Mg/Al mixed oxides led to the incorporation of fluoride anions in various configurations. Overall, the concentration of acid sites was enhanced by this modification while it decreased the concentration of the basic sites. The rate of dehydrogenation of propan-2-ol drastically increased in the presence of F^- anions, but the rate of dehydration was hardly influenced. This indicates that the fluoride anions improve the ability of the mixed oxides to abstract protons from polar molecules without increasing the overall base strength of the mixed oxide.

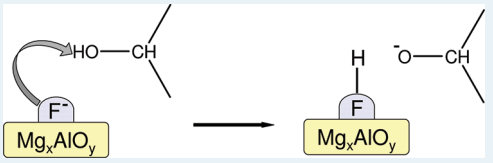

KEYWORDS: Mg/Al mixed oxides, F^- modification, XRD, $^{27}Al/^{19}F$ MAS NMR, dehydrogenation of propan-2-ol

INTRODUCTION

The use of hydrotalcites, layered double hydroxides (LDH), and their derived mixed metal oxides as precursors for solid base catalysts is very attractive because it allows one to subtly adjust the base properties by substitution of various cations.[1] The successful implementation of these catalysts for base-catalyzed reactions, such as aldol condensation, olefin isomerization, Claisen−Schmidt condensation or the Meerwein Ponndorf Verley reduction of aldehydes by alcohols, has been recently extended to catalyze the transesterification of triglycerides as well as other transformations of oxofunctionalized molecules.[2] It should also be mentioned in passing that the direct transformation of CO_2 into organic carbonates also requires tailored solid bases.[3]

The basic properties of mixed oxides (such as hydrotalcites and oxides derived from hydrotalcite) are largely determined by their chemical composition.[4,5] This is related to the fact that the chemical composition in turn determines the intermediate electronegativity, according to Sanderson,[6] which reflects the fact that atoms in a chemical compound redistribute their electrons to equalize the electronegativity of the constituents. The model suggests that, for example, the electron density of the oxygen in an oxide should be a unique function of the intermediate electronegativity, and indeed, this has been shown by XPS.[7] Addition of an element that has a higher electronegativity (such as halogens) thus increases the intermediate electronegativity, whereas elements with a lower electronegativity decreases it. For oxides, higher intermediate electronegativity results in more covalent oxides and lower negative charge at the oxygen and, hence, lower potential base strength and higher potential acid strength (see, e.g., ref 8). In practical terms, this suggests, for example, that increasing the concentration of magnesium over aluminum cations in the corresponding mixed oxide will increase the base strength and decrease the Lewis acid strength.[9−12]

The fact that hydrotalcites are anion exchangers enables a wide range of variations in their chemical compositions. Chloride exchange, for example, has been shown to drastically decrease the basic properties of hydrotalcites.[13] Surprisingly, Wu et al.[14] reported recently that the modification of Mg/Al mixed oxides with fluorine is an effective method to increase their activity in reactions, such as aldol condensation, that are usually catalyzed by solid bases. In addition, however, supported fluoride salts such as KF (KF/alumina) have been reported to have high base strength.[15] This would, in principle, indicate that the base strength of the modified oxides can be increased even though the overall negative charge at the oxygen is decreased.

Because the concept of intermediate electronegativity can be applied only within a given mixed oxide, it is important to understand the presence of various phases in the mixed oxide. In this paper, we explore, therefore, the influence of fluoride anions on the effective acid−base properties of different Mg/Al mixed metal oxides using ^{27}Al, ^{19}F MAS NMR and NH_3 and CO_2 TPD to explore if the overall charge on the oxygen anions is decoupled from the manifested activity in base-catalyzed reactions. The catalytic properties were explored via dehydration and dehydrogenation of propan-2-ol[16−20] and with the condensation of 1,2-epoxyoctane and hexanol, which is usually catalyzed by alkali hydroxides in liquid phase reactions.

Received: April 3, 2011
Revised: July 10, 2011
Published: September 01, 2011

Table 1. Amounts of Mg/Al Mixed Oxide Precursors (calcined at 600 °C) and Concentrations of NH_4F Solution Used for the Synthesis of Fluorinated Mg/Al Mixed Oxides

sample	precursor	m (precursor), g	m (NH_4F), g	V $(NH_4F)_{aqu}$, mL	c $(NH_4F)_{aqu}$, mol·L^{-1}	n $(NH_4F)_{aqu}$, mmol
HT2-F 0.1	HT2	8	2.96	800	0.1	80
HT2-F 0.2	HT2	8	5.93	800	0.2	160
HT4-F 0.1	HT4	8	2.96	800	0.1	80
HT4-F 0.2	HT4	8	5.93	800	0.2	160

EXPERIMENTAL SECTION

Materials. *Mg/Al Mixed Oxide Precursors.* The Mg−Al hydrotalcite mixed oxide precursor with an Mg/Al ratio of 2 was provided by Cognis and is denoted as HT2. A second hydrotalcite precursor with a Mg/Al ratio of 4 (HT4) was prepared using a sol−gel process following the procedure described in ref 21. For this, an acidic aqueous solution of metal nitrates was prepared by dissolving $Mg(NO_3)_2 \cdot 6H_2O$ (123.08 g, 0.48 mol) and $Al(NO_3)_3 \cdot 9H_2O$ (45.01 g, 0.12 mol) in 0.6 L of decarbonized bidistilled water. A second alkaline solution was prepared from NaOH (48.00 g, 1.2 mol) and $NaHCO_3$ (5.04 g, 0.06 mol) in 0.6 L of decarbonized bidistilled water. Both solutions were heated to 75 °C. For precipitation, the nitrate and alkaline solutions were added dropwise to 400 mL of water at 75 °C, giving a pH of 10. The suspension was aged for 3 h at 85 °C under vigorous stirring. After cooling to RT, the gel was filtered and loaded into an autoclave. Hydrothermal synthesis was carried out for 16 h at 80 °C. The gel was washed with 350 mL of bidistilled water until a pH of 7 of the washing water was reached. The white precipitate was freeze-dried and ground.

Both precursor materials were calcined to 600 °C (heating rate 10 °C·min^{-1}) in a flow of 100 mL·min^{-1} synthetic air for 8 h.

Fluorinated Mg/Al Mixed Oxides. An aqueous ammonium fluoride solution was prepared with deionized water, which had been heated to 90 °C for 2 h to remove dissolved CO_2 and carbonates. The NH_4F solution was added to 8 g of the calcined Mg/Al precursor in a 2 L Schlenk flask. The pH was adjusted to 8 using an ammonia solution (25 wt %) as buffer. The mixture was stirred in an inert atmosphere for 48 h at ambient temperature, then the solid was filtered and washed with deionized water until the pH was 7. The solvent was removed by freeze-drying under reduced pressure. The solid was ground and heated to 500 °C (heating rate 10 °C·min^{-1}) in a flow of 100 mL·min^{-1} synthetic air for 8 h.

The used precursor solids and their chemical compositions are compiled in Table 1. The nomenclature of the fluorinated Mg/Al mixed oxides indicates the concentration of the NH_4F_{aq} solution used for the synthesis.

Characterization. The metal contents of Mg/Al mixed oxides and fluorinated Mg/Al mixed metal oxides as well as the fluoride contents were analyzed by atomic absorption spectroscopy (AAS) using a UNICAM 939 AA spectrometer.

Specific surface areas and pore volumes were determined by physisorption of N_2 at 77 K. The measurements were carried out in a PMI automatic BET sorptometer, and the evaluation was done according to the BET theory.

The crystal structure of the precursors and the fluorinated mixed metal oxides were analyzed by XRD using a Philips X'Pert Pro System (Cu Kα 1 radiation, 0.154 nm) at 40 kV/40 mA. The measurements were taken by using a spinner and a 1/6″ slit in the range from 5° or 20° to 70° 2 θ (0.05°/min). The crystallite size was determined by the full-width-at-half-maximum using the Scherrer equation using a standard material for determining the instrument constant.

^{27}Al and ^{19}F MAS NMR measurements were performed on a Bruker AV500 spectrometer (B_0 = 14.1 T) at a spinning rate of 12 kHz. The temperature was adjusted by passing the bearing and drive gas stream through a heat exchanger to 25 °C. The samples were packed in 4 mm ZrO_2 rotors. The resonance frequency of 130.3 MHz was used for the measurements of ^{27}Al MAS NMR. The spectra were recorded as the sum of 2400 scans with a recycle time of 250 ms. A $\pi/12$ pulse (pulse length = 1.0 μs) was applied for excitation. The chemical shift was referenced against an external standard of solid $Al(NO_3)_3$ (δ = −0.54 ppm). For ^{19}F MAS NMR, a resonance frequency of 470.3 MHz was used. The spectra were recorded as the sum of 100 scans with a recycle time of 5.2 ms. A $\pi/12$ pulse (pulse length = 2.3 μs) was applied for excitation. The chemical shift was referenced against an external standard of $CFCl_3$ (δ = 0 ppm).

Temperature-programmed desorption of ammonia (NH_3 TPD) and carbon dioxide (CO_2 TPD) was used to determine the acidic and basic properties of the solid base catalysts. Catalyst samples were activated at 450 °C for 1 h in vacuum. Ammonia was adsorbed at 1 mbar and 100 °C for 1 h, and CO_2 (1 mbar) was adsorbed at 40 °C for 1 h. For desorption, the samples were heated to the corresponding temperature (from 50 to 700 °C for CO_2 TPD and from 100 to 600 °C for NH_3 TPD) at a rate of 10 K·min^{-1}; desorbing gases were monitored with a Pfeifer mass spectrometer. Note that the concentration of sites is calibrated with a H-MFI 90 zeolite and $NaHCO_3$, respectively.

Catalytic Experiments. The as-prepared samples (0.02 g diluted in 0.13 g SiC) were fixed with quartz wool in a quartz-tube reactor with a diameter of 4 mm. The samples were activated by rising the temperature from ambient to 450 °C for 2 h (10 °C·min^{-1}) in a flow of He (20 mL·min^{-1}). The samples were cooled to reaction temperature, and a flow of helium (30, 50, and 70 mL·min^{-1}) saturated with propan-2-ol ($p_{propan\text{-}2\text{-}ol}$ = 25 mbar at 13 °C) was passed over the catalyst. The dehydrogenation/dehydration of propan-2-ol was studied within the temperature range of 225−300 °C using steps of 25 °C. At each reaction temperature, the catalytic reaction was performed for 80 min. Unreacted propan-2-ol and dehydrogenation/dehydration products were analyzed by gas chromatography using a Hewlett-Packard 5890 (series II) GC equipped with a flame ionization detector. The separation of the various components was done by a Q column.

The condensation of 1,2-epoxyoctane with hexanol was performed in a 100 mL flask. Hexanol (2.555 g, 0.025 mol) was added to 1,2-epoxyoctane (4.038 g, 0.026 mol) and heated to 160 °C in a N_2 atmosphere while stirring. The catalyst (0.066 g, 1 wt %) was added, and samples were taken every hour. The catalyst was removed by filtration. The filtrate (100 μL) was mixed with 2,2,4-trimethylpentane (937 μL) as internal standard for GC analysis. The unreacted 1,2-epoxyoctane, hexanol, and

dx.doi.org/10.1021/cs200175x |ACS Catal. 2011, 1, 1384–1393

Table 2. Textural Analysis and Acid−base Properties of Precursors (calcined at 600 °C) and Fluorinated Mg/Al Mixed Oxides (calcined at 500 °C)[a]

					basic sites (μmol·m^{-2})		
sample	Mg/Al (mol/mol)	F content (wt %)	SA_{BET} (m^2·g^{-1})	acid sites (μmol·m^{-2})	weak sites	strong sites	total sites
HT2	2.1		171	0.51	0.060	0.040	0.10
HT2-F 0.1	2.3	9	167	0.46	0.006	0.384	0.39
HT2-F 0.2	2.2	18	186	0.68	0.013	0.377	0.39
HT4	3.8		188	0.15	0.098	0.002	0.10
HT4-F 0.1	3.7	14	162	0.58	0.047	0.003	0.05
HT4-F 0.2	4.0	26	145	0.90	0.009	0.001	0.01

[a] The concentration of acid and basic sites has been calibrated to a standard material.

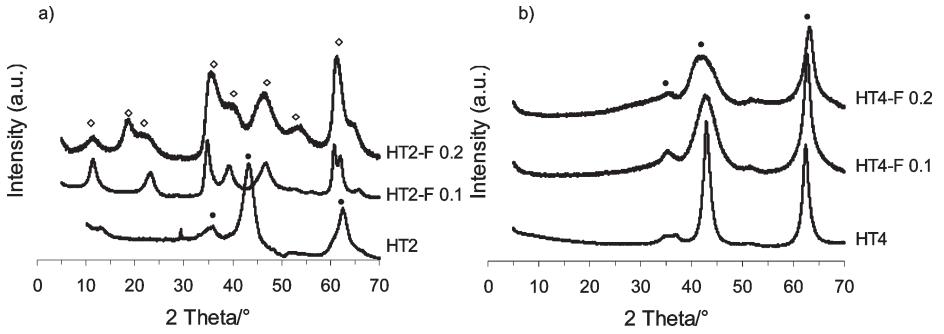

Figure 1. XRD patterns of plain and anion-exchanged Mg/Al mixed oxide samples: (a) HT2 series and (b) HT4 series. ●, MgO (cubic); ◀, $Mg_6Al_2CO_3(OH)_{16}\cdot 4H_2O$.

reaction products were analyzed by gas chromatography using a Shimadzu GC-2010.

RESULTS

Textural Analysis. The metal content, the specific surface areas of the precursors, and the fluorinated Mg/Al mixed oxides are compiled in Table 2. It also includes the concentrations of acid and basic sites determined by CO_2 and NH_3 TPD (see also Section 3.5, and Supporting Information S2 and S3). The specific surface area of the solid base catalyst was hardly influenced when HT2 (Mg/Al = 2.0) was fluorinated with a 0.1 M ammonium fluoride solution (HT2 = 171 m^2·g^{-1}; HT2-F 0.1 = 167 m^2·g^{-1}). When the sample was treated with a higher concentration of ammonium fluoride, the specific surface area of HT2 increased to 186 m^2·g^{-1}.

For HT4, the specific surface area decreased from 188 to 162 m^2·g^{-1} and to 145 m^2·g^{-1} for HT4-F0.1 and HT4-F0.2, respectively. For both oxides, the fluoride content was also doubled by treatment with a 0.2 M NH_4F_{aq} solution, as compared with the 0.1 M solution. Overall, the fluoride content of fluorinated HT4 was, however, higher compared with fluorinated HT2.

XRD Analysis. The XRD patterns of the Mg/Al mixed oxides (HT2 and HT4) and the F^--exchanged samples are compiled in Figure 1. The diffraction peaks of MgO were observed at 2θ = 35.6, 43.0, and 62.5°; those of hydrotalcite, at 2θ = 11.7, 23.4, 35.0, 39.7, 47.0, 53.9, and 61.5°.

The pattern of calcined HT2 was dominated by cubic MgO, whereas after fluorination, the hydrotalcite structure was found. Such reconstruction of the hydrotalcite structure has been described by Tichit et al.,[6] who obtained meixnerite (LDH structure) from a previously calcined Mg(Al)O spinel. Note that in their case, the reconstruction ability was enhanced by using a lower calcination temperature. Because the widths of the peaks in all diffractograms were very broad, we conclude that the samples have low crystallinity. The primary crystallite size was estimated to be 6−7 nm.

The diffraction peaks of HT4 and fluorinated HT4 samples corresponded to cubic MgO. In the fluoride exchanged samples, a broadening of the peak at 43.0° was observed, indicating a distortion of the MgO phase. It should be emphasized that indications of a restitution of a layered structure were not observed for the fluoride-treated HT4 sample.

The structural transformation of HT4 from the LDH precursor to the mixed oxide was followed by in situ XRD analysis from RT to 600 °C in a flow of 5 mL·min^{-1} synthetic air. The results are illustrated in the Supporting Information, section S1. At RT, the main diffraction peaks were observed at 2θ = 11.4, 23.0, 34.7, 38.6, 45.6, 60.4, 61.5, and 65.6° related to the hydrotalcite structure with the general molecular formula of $Mg_6Al_2CO_3(OH)_{16}\cdot H_2O$. At 200 °C, the intensity of the diffraction peaks decreased, and their widths increased. This indicates smaller domains of the HTC structure and, hence, indicates the structural transformation from hydrotalcite to Mg_xAlO_y. Further temperature increase to 400 °C resulted in a complete transformation to Mg_xAlO_y. Between 400 and 600 °C, further changes of the structure were not observed by XRD.

^{27}Al MAS NMR Spectroscopy. MAS NMR spectroscopy of the solid materials was used to identify changes in the crystal structure after fluorination of the Mg/Al mixed oxides. The ^{27}Al MAS NMR spectra of HT2, fluorinated HT2 (a) and HT4 and fluorinated HT4 (b) are compiled in Figure 2. The chemical

dx.doi.org/10.1021/cs200175x |ACS Catal. 2011, 1, 1384–1393

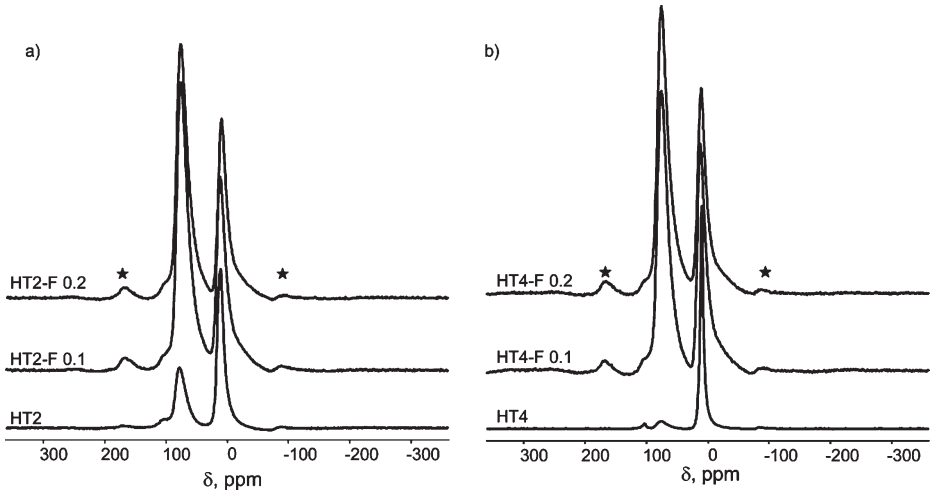

Figure 2. ^{27}Al MAS NMR of plain and anion exchanged Mg/Al mixed oxide samples: (a) HT2 seriesand (b) HT4 series. ★, satellite signals.

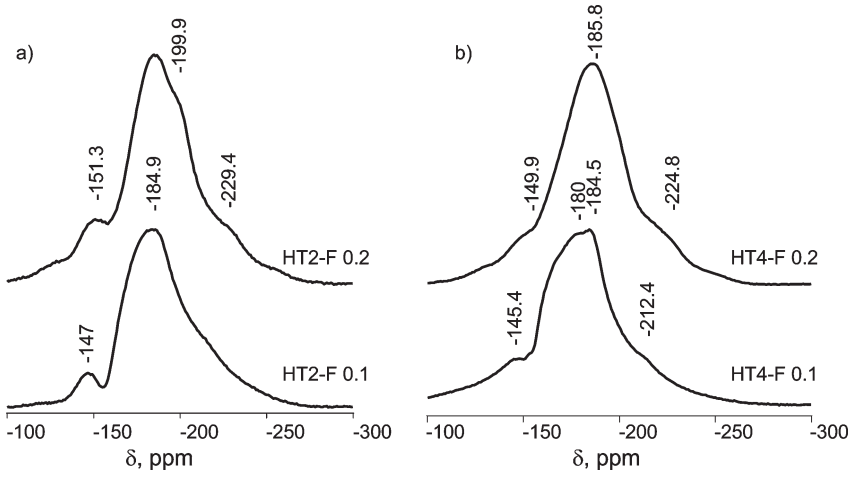

Figure 3. ^{19}F MAS NMR of plain and anion-exchanged Mg/Al mixed oxide samples: (a) HT2 series and (b) HT4 series.

shifts of octahedrally and tetrahedrally coordinated Al are located at ∼11 and 75 ppm, respectively.[22,23] In the case of HT2, tetrahedrally and octahedrally coordinated aluminum species were found, but the fluorinated HT2 samples showed a marked increase of the signal related to tetrahedral aluminum.

In comparison with the ratio of intensities observed with HT2, the peak of tetrahedral aluminum in HT4 was very small compared with the octahedral aluminum species. Similar to the results for fluorinated HT2, the peak at 75 ppm increased after fluorination for HT4. Although the ratio between tetrahedral and octahedral alumina species increased from 0.62 (HT2) to 1.85 for HT2-F 0.2, the conversion of octahedral to tetrahedral alumina was even more pronounced for HT4; that is, it increased from 0.09 (HT4) to 1.82 for HT4-F 0.2. It is interesting to note that the tetrahedral/octahedral ratios for HT2-F and HT4-F were almost identical (1.82 and 1.85, respectively). For both precursor materials, a distinct broadening of the high field signal at 10 ppm toward higher field was observed for the fluorinated samples, which increased with increasing fluoride content, indicating a distinct impact of the fluoride anions.

^{19}F MAS NMR Spectroscopy of Fluorine-Modified Mg/Al Mixed Oxides. All ^{19}F MAS NMR spectra of fluorinated Mg/Al mixed oxides are dominated by one main signal at approximately −184 ppm (see Figure 3). The signal is attributed to a MgF_2-type species adjacent to oxygen atoms.[24] Furthermore, in the case of HT2-F0.1, a broad shoulder at −147 ppm was observed. With an increasing degree of fluorination of HT2-F, this shoulder shifted to −151.3 ppm. It is attributed to F^- coordinating to aluminum cations. This high-field shift was also observed by Zhang et al.[25] for higher fluorine contents.

Two additional small shoulders at −199.9 and −229.4 ppm were observed for HT2-F0.2. According to Prescott,[5] a terminal F^- coordinated to Mg is expected at −200 ppm, and a bridging fluoride with a Mg−F distance of 1.7 Å should be observed at −218 ppm. Thus, we tentatively ascribe the shoulders to these surface species.

For Mg/Al mixed oxides with higher magnesium concentrations (HT4), the signals attributed to bridging Al−F structures were observed at −145.4 (HT4-F0.1) and 149.9 ppm (HT4-F0.2). Note that compared with HT2, the Al−F signals were shifted to lower field. The Mg−F signals were observed at −184.5 (HT4-F0.1) and −185.8 ppm (HT4-F0.2). In the case of the lower fluoride content, an additional signal was observed at −180 ppm. This resonance is attributed to a second, highly

dx.doi.org/10.1021/cs200175x |ACS Catal. 2011, 1, 1384–1393

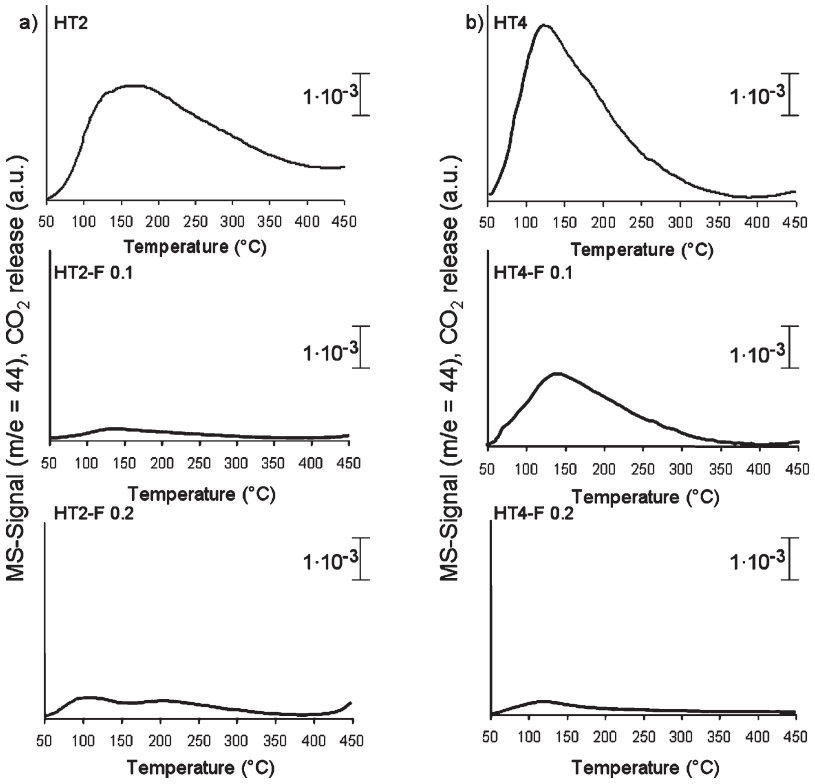

Figure 4. CO_2 TPD of parent and F^- modified Mg/Al mixed oxides.

diluted Mg−F species, as described by Reinholdt et al.[26] The high field signal at <−200 ppm occurred at −212.4 ppm for HT4-F0.1 and was shifted to −224.8 ppm with increasing fluorine content. In both cases, a fluoride anion is suggested to assume a bridging position between two Mg^{2+} cations.

Base Properties Determined by TPD of CO_2. The desorption profile of HT2 (Figure 4) shows a broad, structured peak with a maximum at temperatures below 350 °C as well as a more narrow desorption peak at 550 °C (see the Supporting Information for temperatures above 450 °C). According to the two desorption maxima in the CO_2 TPD, the basic sites are classified as weak (W) and strong (S) sites (see Table 2). After modification with fluoride anions, the more intense low-temperature maximum disappeared, and the high temperature desorption peak broadened and markedly grew in intensity for HT2-F0.1 and HT2-F0.2. Note that the desorption maximum of the high temperature peak was found at higher temperatures for HT2-F0.1 compared with HT2-F0.2

With HT4, fluorination hardly changed the overall appearance of the desorption profile. Desorption of CO_2 occurred at temperatures below 350 °C. In comparison with the HT2-modified samples, only a small fraction of CO_2 molecules desorbed at temperatures above 450 °C. Also in this case, the concentration of desorbed CO_2 decreased with the severity of fluoride addition.

Kinetics of Elimination Reactions of Propan-2-ol. The catalytic properties of the Mg/Al mixed oxides and their fluoride-modified derivatives were explored with respect to the elimination reactions of propan-2-ol. Generally, propene is formed via dehydration on catalysts with dominating acid sites, whereas acetone is formed as the main dehydrogenation product when basic sites are dominating. The selectivity to propene and acetone has therefore been traditionally used as an indicator of the acidic or basic properties of mixed oxides, in addition to TPD of NH_3 and CO_2.

The TOF of acetone formation (see Table 3 and Figure 6) increased for both series of materials with increasing fluoride content. In contrast, the TOF for the dehydration decreased slightly (HT2 series) or hardly changed (HT4 series). The increase in the TOF for dehydrogenation was accompanied by a nearly constant apparent energy of activation of 107 ± 12 kJ/mol. The apparent energies of activation for dehydration hardly changed (83 kJ/mol). With HT4, the apparent energy of activation for propan-2-ol dehydrogenation was slightly lower (97 ± 8 kJ/mol), and the apparent energy of activation for dehydration again was 85 ± 8 kJ/mol.

The yield−conversion plots for Mg/Al mixed oxides and fluorinated samples at 275 °C are shown in Figure 6. The selectivity toward dehydrogenation for HT2 was 27% and increased with increasing content of fluorine to 60% (HT2-F 0.1) and 82% (HT2-F 0.2). For HT4, the selectivity to acetone increased with fluorination from 54 to 90% (HT4-F 0.1). The straight lines show that none of the products undergoes secondary reactions to a significant extent.

Catalytic Condensation of 1,2-Epoxyoctane with Hexanol. Ring-opening reactions of epoxides are useful routes in organic synthesis of allylic and aliphatic compounds catalyzed by acids and bases.[27−29] The reaction of 1,2-epoxyoctane (1) with hexanol (2) is a nucleophilic substitution in which the alcohol acts as the nucleophile and 1-(hexyloxy)octane-2-ol (3) is formed as the main product. The reaction scheme of the nucleophilic ring-opening reaction of the epoxide is shown in Figure 7.

The catalytic performance of Mg/Al mixed oxides and fluorine-modified Mg/Al oxides during the ring-opening reaction of

dx.doi.org/10.1021/cs200175x |ACS Catal. 2011, 1, 1384–1393

Table 3. Conversions of Propan-2-ol, Selectivities to Acetone/Propene and Turnover Frequencies[a] of Acetone Formation, Basic/Acid Ratios of Mg/Al and Anion-Exchanged Mixed Metal Oxides

sample	conversion (%), propan-2-ol	selectivity (%), acetone	TOF (s^{-1}), acetone	TOF (s^{-1}), propene	E_a ($kJ \cdot mol^{-1}$), acetone	E_a ($kJ \cdot mol^{-1}$), propene
HT2	4	27	3.9	1.3	118	91
HT2-F 0.1	1	60	36.7	0.3	115	83
HT2-F 0.2	5	82	81.3	0.3	95	91
HT4	9	54	0.9	0.5	89	95
HT4-F 0.1	9	90	55.5	0.5	91	95
HT4-F 0.2	6	75	167.2	0.7	105	77

[a] TOF was determined by using the weak basic site density for acetone and the acid site density for propene at a temperature of 275 °C and a flow of 50 $mL \cdot min^{-1}$.

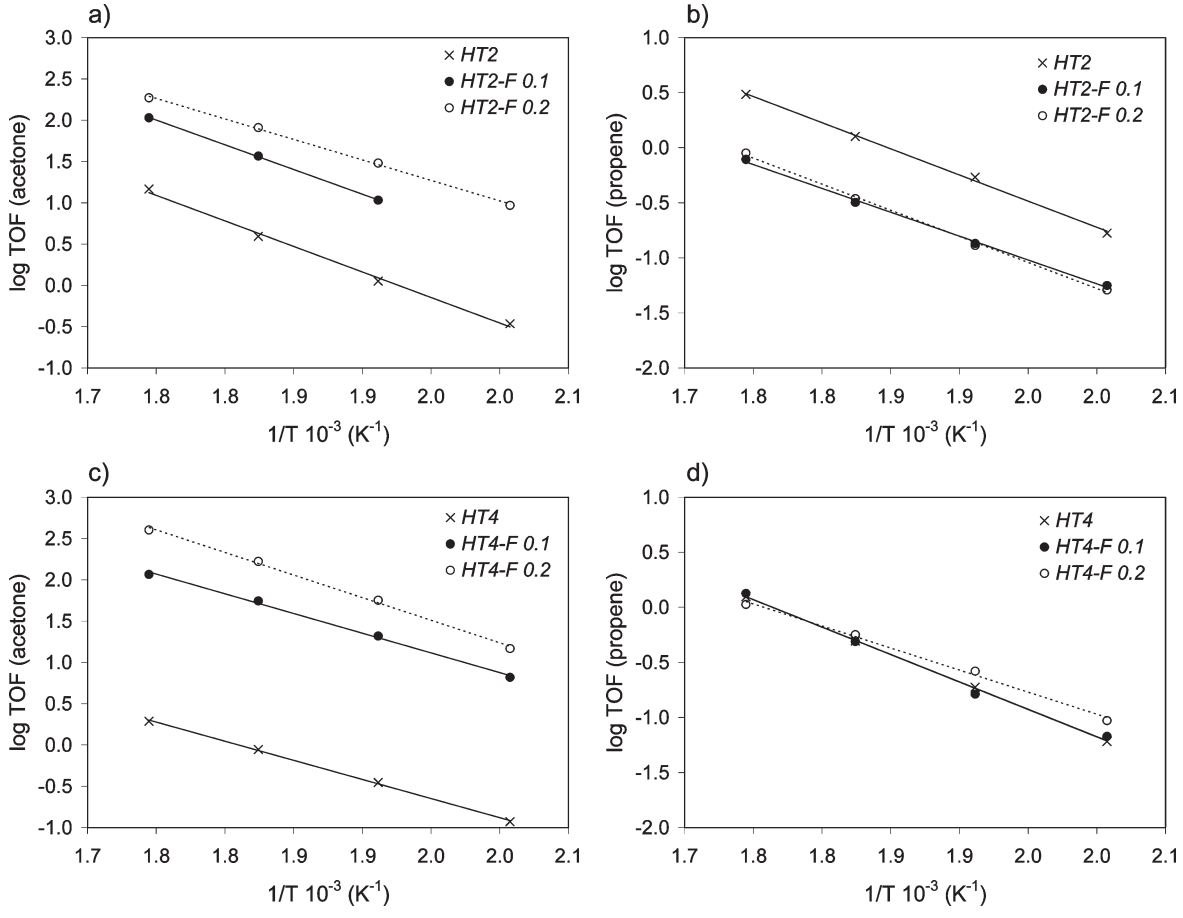

Figure 5. Turnover frequency of product formation from propan-2-ol conversion as a function of the inverse temperature for various Mg/Al and F-modified Mg/Al mixed oxide samples. HT2 and fluorinated HT2: (a) formation of acetone and (b) formation of propene. HT4 and fluorinated HT4: (c) formation of acetone and (d) formation of propene.

1,2-epoxyoctane with hexanol at 160 °C is compiled in Figure 8. In the series of fluoride-modified catalysts, the yield of 1-(hexyloxy)octane-2-ol decreased with increasing concentration of fluorine. The decrease in activity due to fluorination was significantly higher in the case of HT2 compared with HT4. Although the yield of 1-(hexyloxy)octane-2-ol was 63% for HT2, it dropped to less than 10% for fluorinated HT2. In comparison, for HT4, only a slight decrease in activity from 76 to 67% was observed for HT4-F0.1. A further decrease to 51% was observed for HT4-F0.2. The high selectivity (>75%) to the target reaction was maintained in both cases.

DISCUSSION

Fluorinated Mg/Al mixed oxides were prepared in this study to explore the impact of fluoride anions on the acid−base and the catalytic properties of magnesium−aluminum mixed oxides. Although the parent and the fluorided samples show the expected

dx.doi.org/10.1021/cs200175x |ACS Catal. 2011, 1, 1384–1393

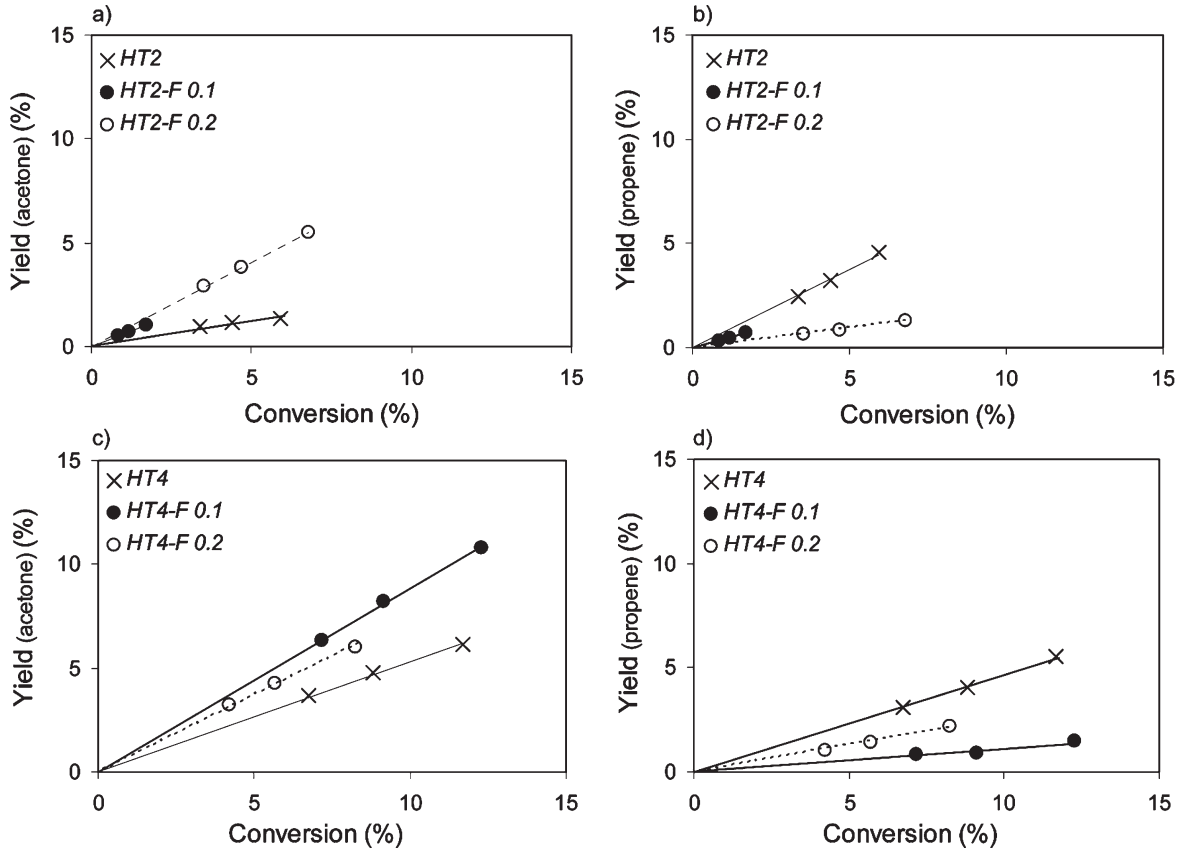

Figure 6. Yield conversion plots of propan-2-ol dehydrogenation and dehydration under variation of the He/propan-2-ol flow (30, 50, and 70 mL/min) for precursors (calcined at 600 °C) and fluorinated Mg/Al mixed oxides (calcined at 500 °C) at 275 °C. HT2 and fluorinated HT2: yield of (a) acetone and (b) propene. HT4 and fluorinated HT4: yield of (c) acetone and (d) propene.

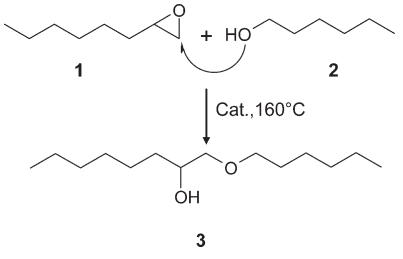

Figure 7. Reaction scheme of the nucleophilic ring-opening reaction of 1,2-epoxyoctane with hexanol.

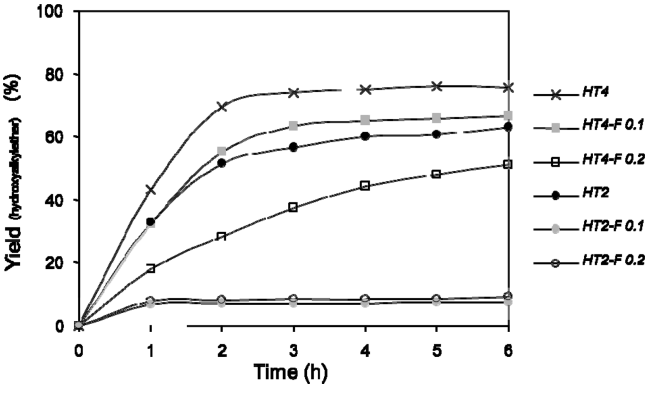

Figure 8. Yield of 1-(hexyloxy)decane-2-ol with F-modified and Mg/Al mixed oxides (T = 160 °C).

mutual impact of the acidic (alumina) and the basic (MgO) component,[30,8] the subtle effects were seen to depend on the local structures induced by the different precursor structure and chemical composition (HT2 had a Mg/Al ratio of 2.1; HT4, 3.8). With the differing concentration of the two main chemical constituents in the corresponding precursors, one notes that with the higher Mg content, MgO became the dominating phase. This indicates that the higher MgO content either led to the formation of very small X-ray amorphous domains of hydrotalcite or it suppressed its formation entirely. That latter possibility is in agreement with the lack of a high-temperature peak in TPD of CO_2, which is associated with the decomposition of the layered carbonate. The aqueous phase treatment with fluoride led to the formation of the hydrotalcite structure with HT2. This is attributed to the reconstruction of LDHs by treatment in aqueous solutions (possibly aided by the presence of fluoride anions and calcination at lower temperatures) described also as the memory effect.[6] For HT4 and fluorinated HT4, samples crystallized only in the MgO or a MgO-dominated Mg_xAlO_y mixed phase similar to the material reported also by Wu et al.[14] The differences in the structural changes of HT2 and HT4 due to the treatment in aqueous NH_4F solution are tentatively explained by the influence of the preparation method on the memory effect of LDH compounds. Dávila et al.[31] reported that a memory effect strongly depends on the preparation method and rehydration/calcination

dx.doi.org/10.1021/cs200175x |ACS Catal. 2011, 1, 1384–1393

cycles of the layered double hydroxide precursors. At present, we speculate that the difference between the structural behaviors of the two samples is related to the different chemical compositions and variations in the material preparation. The ^{27}Al MAS NMR results indicate that the nature of incorporation of aluminum in HT4 and HT2 also varies, indicating marked differences in the starting materials.

There was no linear trend observable for changes in the specific surface areas of HT2 with increasing degree of fluoridation, whereas the specific surface area of HT4 decreased with an increasing concentration of fluoride. Using ^{27}Al MAS NMR, octahedral and tetrahedral alumina species were identified in both materials (HT2 and HT4). A significant increase in tetrahedral alumina is observed after fluorination, which was more pronounced for HT4 than for HT2. Note that the transformation of 6-fold-coordinated to 4-fold-coordinated Al after several rehydration/calcination steps by ^{27}Al MAS NMR was also observed by Dávila et al.[31] We concluded that this transformation is associated with phase separation of an alumina-rich oxide phase. It should be emphasized that the domains of the phase must be small because XRD does not indicate the presence of a crystalline alumina phase.

The broadening toward higher field of the peak at 10 ppm for all fluorinated samples is attributed to a partial substitution of oxygen by fluorine in the vicinity of aluminum. Similar observations were found by König,[32] who explored the local structural changes of aluminum isopropoxides by fluorine.

The fluoride species were identified via ^{19}F MAS NMR using the five differently coordinated fluorine types potentially present in the solid catalyst.[24−26,33] The main signal in the NMR spectrum of HT2-F0.1 is attributed to a MgF_2 species; the sharp shoulder at −147 ppm, to octahedral AlF_xO_y. We concluded that for HT2-F0.2, two additional signals of fluorine coordinated to magnesium, characteristic for terminal and bridging Mg−F structures are present. In comparison with HT2-F0.1, the intensity of the Al−F related signal is smaller, but shifted to a higher field (−151 ppm). The shift of the signal of HT2-F0.2 related to Al−F indicates a higher polarization of the Al−F bond toward the fluorine atom. Thus, the electron density is redistributed toward the fluorine atom in HT2-F0.2, which should lead to a higher positive charge at the metal cations, that is, a higher potential Lewis acid strength.

Similar to the spectrum of fluorinated HT2, the NMR spectrum of fluorinated HT4 was dominated by MgF_2. However, in the spectrum of HT4-F0.1, an additional Mg−F species was observed. This additional Mg−F species resembles more a terminal than a bridging Mg−F structure. In contrast, the Mg−F species observed in HT4-F0.2 resembles more a bridging Mg−F. The same trend with respect to the polarization of the Al−F bond as for fluorinated HT2 was observed. With increasing fluorine content, the signal of Al-bound F was shifted from −145 to −150 ppm, indicating high polarity for HT4-F0.2.

The two desorption maxima of CO_2 suggest sites that weakly stabilize absorbed CO_2 as well as sites that are able to stabilize CO_2 up to high temperatures. Although this is, per se, indicative of sites with different base strengths, we would like to emphasize that the maximum at high temperatures is associated with the decomposition of the hydrotalcite and the release of CO_2 from carbonate anions, which are apparently stabilized in the partly anion-exchanged hydrotalcite structure.

The concentration of weak basic sites, which are relevant for catalysis, markedly decreased by the modification of HT2 with fluorine, and the concentration of strong basic sites distinctly increased. We conclude that the increase in sites retaining CO_2 up to high temperatures ("strong basic sites") is caused by the formation of the hydrotalcite structure after fluoride treatment. In comparison with the calcined precursor, the concentration of basic sites decreased with fluoride modification for HT4. Note that with HT4, hydrotalcite was not formed after treatment with fluoride anions. Although this decrease is moderate for HT4-F0.1, that is, a factor of 2, it was very pronounced for HT4-F0.2. The decreased basicity after fluoride treatment is explained by a lower fraction of basic oxygen through the enrichment of F^- on the surface or the formation of MgF_2 surface domains.[18] This suggests that a significant fraction (especially the most reactive ones) of the surface oxygen anions and hydroxyl groups have been exchanged for fluoride anions, which interact only weakly with CO_2.

Such an exchange is in agreement with the increase in the concentration of moderately strong acid sites (i.e., accessible Mg^{2+} cations), as discussed below. The higher electronegativity and smaller ionic radius of F^- compared to O^{2-} lead to a better accessibility and a higher acid strength of the cations. Note that in contrast to MgO, aluminum cations are preferentially tetrahedrally coordinated after fluoride modification in both materials and in that way are better shielded than in the starting material. The concentration of acid sites, as determined by desorption of ammonia, shows an almost identical surface-averaged concentration of sites for materials with the increasing concentration of fluoride anions. Not only does this suggest very similar surface structures (considering the overall difference in chemical composition between Mg and Al cations), it also shows that the modification was dominating the surface structure. In both cases, the increase in acid site concentration is attributed to the increase in coordinatively unsaturated Mg^{2+} and/or Al^{3+} cations.

Thus, judging from the sorption/desorption of probe molecules, the modification of the $MgO-Al_2O_3$ mixed oxide with fluoride anions leads to heterogeneous samples. The influence of fluorination on strong basic sites varies with varying Mg/Al ratios. The concentration of strong basic sites (attributed to a stabilization of carbonate ions via thermal stabilization of the hydrotalcite structure) is increased for the sample with a lower Mg/Al ratio, whereas for the samples with the higher Mg/Al ratio, the changes in the strong basic sites were marginal (the hydrotalcite structure was not formed in the modification procedure). The concentration of weak base sites (attributed to coordinatively unsaturated surface oxygen and hydroxyl groups) is decreased in both cases. In parallel, the concentration of weak acid sites increases, which we concluded is caused by a better accessibility of the cations, which is caused by the partial replacement of the oxygen and hydroxide anions by the smaller anion F^-.

Given that overall picture of the modification of the acid−base properties, let us analyze the conversion of propan-2-ol, which is generally claimed to be an indicator for the effective acid and base properties of the mixed oxide/fluoride catalysts. The TOF for the formation of acetone increased with the fluoride content (see Figure 9a), while the formation of propene was unaffected (see Figure 9b). Thus, the fluoride treatment of the samples caused the modified Mg/Al mixed oxide to act like a more basic catalyst (higher TOF for dehydrogenation) while the results of characterization did not indicate variation basic sites that could participate in the reaction.

The apparent discrepancy between the variation of the acid−base properties measured by probe molecules and the catalytic

dx.doi.org/10.1021/cs200175x |ACS Catal. 2011, 1, 1384–1393

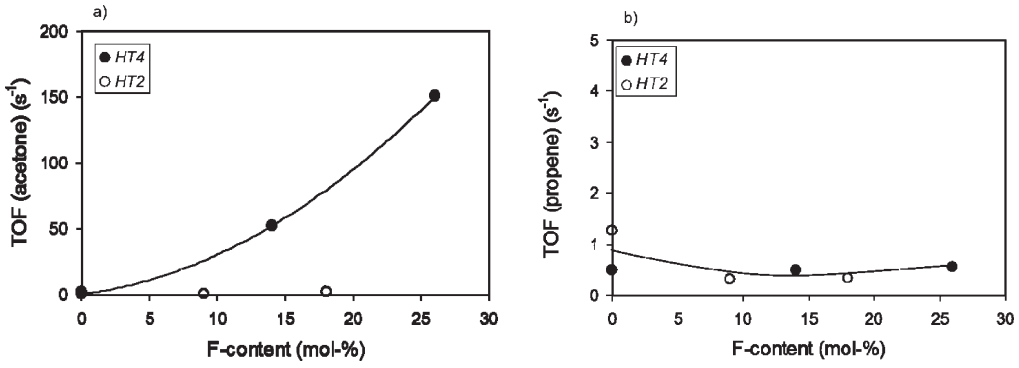

Figure 9. TOFs of product formation of propan-2-ol conversion depending on the fluorine content at 275 °C and 50 mL·min^{-1} gas flow (varying conversion; see Table 3) for various Mg/Al mixed oxide samples: (a) formation of acetone and (b) formation of propene.

performance can be understood via the three elementary reaction steps of dehydrogenation (and dehydration) of propan-2-ol. In the first step, the alcohol adsorbs dissociatively on an acid−base pair, that is, the alcohol O−H bond cleaves, forming an OH group with basic oxygen, while the alkoxide is stabilized by the metal cation. In the second step, a hydride is abstracted from the alkoxide by another accessible acid site. The third step includes the recombination of two H atoms to form dihydrogen and the desorption of acetone into the gas phase. It should be noted that this sequence can occur simultaneously (concerted mechanism) or in steps (ionic mechanism). Because the oxygen anions are not to be expected to increase in electron density by adding fluoride anions, we conclude that the fluoride anion specifically facilitates the proton abstraction from the alcohol hydroxy group. Together with the larger concentration of accessible metal cations, the conclusion is that the more facile proton abstraction enhances the rate of formation of the alkoxy groups.

It is interesting to mention that a related observation by Wu et al.,[14] was explained by the more facile activation of phenol on Mg−F pairs and F^- than on the Mg−O pairs and O^{2-}. The hydrogen bonding to the fluoride anion (25−40 kJ/mol) was significantly stronger than that to the oxygen anion (13−29 kJ/mol).

We speculate that the transiently formed HF is rapidly hydrolyzed by OH groups (forming water and F^-) or participates in forming H_2 at a coordinatively unsaturated Mg^{2+} site binding H^-. Although the stable catalyst behavior points to the fact that the former reaction is limited in extent, the current data do not allow speculation with respect to the rates at which such reactions occur. The quite constant apparent energies of activation point to the fact that the increase in the rate rather enhances one of the reaction steps in quasi equilibrium (by stabilizing a higher equilibrium concentration of an intermediate) and not the rate-determining step.

In contrast to dehydrogenation, the fluorine coordination surprisingly does not accelerate the dehydration of propan-2-ol. We conclude that the higher concentration of acid sites (accessible Mg^{2+} cations) did not lead to an enhanced rate of cleavage of the C−O bond. Because the overall concentration of the acid sites is increased in the modified samples, we concluded that the higher concentration of fluoride anions negatively influences the stabilization of the propyl carbenium ion. Because the formation of fluoro alkanes has not been observed, the interaction between the propyl carbenium ion and the fluoride anion must be very weak. Thus, the interaction of the carbenium ion with the more compact F^- anion is much weaker than with the more polarizable O^{2-} anion.

Like the dehydrogenation of propan-2-ol, the ring-opening reaction of an epoxide with an alcohol, specifically, the reaction of 1,2-epoxyoctane with hexanol to 1-(hexyloxy)decane-2-ol, appears to be catalyzed by moderately strong bases. Also in this case, the modification with fluoride anions had a negative impact on the catalytic activity. Although a higher concentration of Mg^{2+} in the mixed oxide is positive for the rate (HT4 was more active than HT2), the substitution of oxygen with F^- in the surface reduced the rate. We concluded that this decrease in the rate is caused by the higher stability of the F−H bond compared with O−H bond. In the first step of the reaction sequence, the alcohol is deprotonated by a basic site. This is followed by a nucleophilic attack of the alcoholate on the unsubstituated α-C-atom of the epoxide. Subsequently, the ring is opened, and a proton is abstracted from the surface of the catalyst. Because the F−H bond is stronger than the O−H bond, the presence of F^- anions may facilitate the first reaction step and in turn significantly retard the abstraction of protons from the surface. The fact that the overall rate decreased by the addition of fluoride anions indicates that this latter step determines the overall formation rate of 1-(hexyloxy)octane-2-ol.

CONCLUSIONS

Mg/Al mixed oxides derived from LDH precursors were modified with fluoride to study the much-claimed positive impact on their basic properties. The fluoride modification led to a substitution of surface oxygen atoms and hydroxyl groups by F^- anions as well as to an increase in the concentration of Lewis acid sites (unsaturated Mg cations). With some of the materials, the presence of fluoride in the materials led to a surprising stabilization of the hydrotalcite structure, without changing the impact of the fluoride substitution. This stabilization led, however, to the stabilization of carbonate ions in that structure.

The presence of F^- anions does not lead to a better stabilization of the reversibly adsorbed CO_2, indicating a lower concentration of accessible basic sites. We concluded that the higher concentration of unsaturated cations is due to the presence of the smaller and more compact F^-.

The differences in the catalytic performance reflect the influence of the particular properties of the fluoride anions. Although they seem to enhance the proton-accepting properties, probably by generating a transiently stable HF species, and

thus lead to the stabilization of secondary propoxy groups by accessible Mg^{2+} cations, the stabilization of the more polarizable sec propyl carbenium ions is not improved. This leads to an increase in the dehydrogenation, which is, in this case, not an indication of a higher base strength. Similarly, the ring-opening of an epoxide by reaction with an alcohol is retarded because the reaction requires a subtle balance of proton acceptance and donation from the surface, and the presence of F appears to facilitate the former step and makes the latter more difficult.

Overall, the introduction of F^- anions into alumina−magnesia mixed oxides improves their ability to abstract protons from polar molecules in catalyzed reactions. Surface chemical processes that require other stabilizations by basic species, such as the formation of reversible surface carbonates, are not enhanced by the presence of fluoride anions.

■ ASSOCIATED CONTENT

Supporting Information. Additional information as noted in the text. This material is available free of charge via the Internet at http://pubs.acs.org.

■ AUTHOR INFORMATION

Corresponding Author

*Phone: +49-89-289-13540. Fax: +49-89-13544. E-mail: johannes.lercher@ch.tum.de.

■ ACKNOWLEDGMENT

The authors acknowledge fruitful discussions in the framework of the network of excellence IDECAT. Xaver Hecht and Martin Neukamm are acknowledged for their experimental support.

■ REFERENCES

(1) Valente, J. S.; Figueras, F.; Gravelle, M.; Kumbhar, P.; Lopez, J.; Besse, J. P. *J. Catal.* **2000**, *189*, 370–381.
(2) Sivasamy, A.; Cheah, K. Y.; Fornasiero, P.; Kemausuor, F.; Zinoviev, S.; Miertus, S. *ChemSusChem.* **2009**, *2*, 278–300.
(3) Dai, W. L.; Luo, S. L.; Yin, S. F.; Au, C. T. *Appl. Catal., A* **2009**, *366*, 2–12.
(4) Figueras, F. *Top. Catal.* **2004**, *29*, 189–206.
(5) Prescott, H. A.; Li, Z. J.; Kemnitz, E.; Trunschke, A.; Deutsch, J.; Lieske, H.; Auroux, A. *J. Catal.* **2005**, *234*, 119–130.
(6) Sanderson, R. T. *Chemical Bonds and Bond Energy*; Academic Press: New York, 1971.
(7) Vinek, H; Noller, H.; Ebel, M.; Schwarz, K. *J. Chem. Soc., Faraday Trans. I* **1977**, *73*, 734–746.
(8) Lercher, J. A.; Noller, H. *J. Catal.* **1982**, *77*, 152–158.
(9) Lercher, J. A. *Z. Phys. Chem. NF* **1982**, *129*, 209–218.
(10) Lercher, J. A.; Colombier, Ch.; Noller, H. *Z. Phys. Chem. NF* **1982**, *131*, 111–122.
(11) Lercher, J. A. *React. Kinet. Catal. Lett.* **1982**, *20*, 409–413.
(12) Lercher, J. A.; Colombier, Ch.; Noller, H. *J. Chem. Soc. Faraday Trans. I* **1984**, *80*, 949–959.
(13) Tichit, D.; Coq, B. *CATTECH* **2003**, *7*, 206–217.
(14) Wu, G. D.; Wang, X. L.; Chen, B.; Li, J. P.; Zhao, N.; Wei, W.; Sun, Y. H. *Appl. Catal., A* **2007**, *329*, 106–111.
(15) Hattori, H. *Chem. Rev.* **1995**, *95*, 537–558.
(16) Gervasini, A.; Fenyvesi, J.; Auroux, A. *Catal. Lett.* **1997**, *43*, 219–228.
(17) Waugh, K. C.; Bowker, M.; Petts, R. W.; Vandervell, H. D.; O'Malley, J. *Appl. Catal.* **1986**, *25*, 121–128.
(18) Bowker, M.; Petts, R. W.; Waugh, K. C. *J. Catal.* **1986**, *99*, 53–61.
(19) Halasz, I.; Vinek, H.; Thomke, K.; Noller, H. *Z. Phys. Chem. NF* **1985**, *144*, 157–163.
(20) Ouqour, A.; Coudurier, G.; Vedrine, J. C. *J. Chem. Soc., Faraday Trans.* **1993**, *89*, 3151–3155.
(21) Greenwell, H. C.; Holliman, P. J.; Jones, W.; Velasco, B. V. *Catal. Today* **2006**, *114*, 397–402.
(22) Wang, Y.; Han, X. W.; Ji, A.; Shi, L. Y.; Hayashi, S. *Microporous Mesoporous Mater.* **2005**, *77*, 139–145.
(23) Schilling, P. J.; Butler, L. G.; Roy, A.; Eaton, H. C. *J. Am. Ceram. Soc.* **1994**, *77*, 2363–2375.
(24) Prescott, H. A.; Li, Z. J.; Kemnitz, E.; Deutsch, J.; Lieske, H. *J. Mater. Chem.* **2005**, *15*, 4616–4628.
(25) Zhang, W. P.; Sun, M. Y.; Prins, R. *J. Phys. Chem. B* **2002**, *106*, 11805–11809.
(26) Reinholdt, M.; Miehe-Brendle, J.; Delmotte, L.; Tuilier, M. H.; le Dred, R.; Cortes, R.; Flank, A. M. *Eur. J. Inorg. Chem.* **2001**, 2831–2841.
(27) Chidwood, H. C.; Freure, B. T. *J. Am. Chem. Soc.* **1946**, *68*, 680–683.
(28) Parker, R. E.; Isaacs, N. S. *Chem. Rev.* **1959**, *59*, 737–799.
(29) Mirkhani, V.; Tangestaninejad, S.; Yadollahi, B.; Alipanah, L. *Tetrahedron* **2003**, *59*, 8213–8218.
(30) Noller, H.; Lercher, J. A.; Vinek, H. *Mater. Chem. Phys.* **1988**, *18*, 577–593.
(31) Davila, V; Lima, E.; Bulbulian, S.; Bosch, P. *Microporous Mesoporous Mater.* **2008**, *107*, 240–246.
(32) König, R.; Scholz, G.; Kemnitz, E. *J. Phys. Chem. C* **2009**, *113*, 6426–6438.
(33) Kao, H. M.; Chen, Y. C. *J. Phys. Chem. B* **2003**, *107*, 3367–3375.